



## Investigating the Effects of Blockage Ratio on the Performance of a Surface-piercing Propeller in Free Surface Water Tunnel Tests

M. Beykani, R. Shafaghat\*, A. Yousefi

Sea-Based Energy Research Group, Babol Noshirvani University of Technology, Babol, Iran

### PAPER INFO

#### Paper history:

Received 25 November 2022

Accepted in revised form 30 December 2022

#### Keywords:

Efficiency gradient

Experimental study

Hydrodynamic coefficient

Immersion ratio

Surface piercing propeller

### ABSTRACT

This paper investigates the effect of the immersion ratio parameter on the hydrodynamic performance of three surface-piercing propellers with diameters of 0.125, 0.132 and 0.140m at different advancing speeds. Experimental tests have been carried out in the free surface water tunnel of the Babol Noshirvani University of Technology. The results showed that the maximum thrust coefficient of three propellers occurs in the velocity range of 3-3.5 m/s. This interval represents the transition area of the three propellers. Also, the effect of the blockage ratio on the hydrodynamic coefficients of three propellers relative to the advance coefficient has been studied. By increasing the immersion depth raises the propeller's wet surface and increases the thrust and torque hydrodynamic coefficients. However, growing the propeller's diameter to 0.140m causes the effect of the blockage ratio parameter by increasing the immersion and the propeller's torque experiences a decreasing trend. Therefore, maximum propeller efficiency value with diameter 0.140m in immersion ratio 0.60 and 0.70, increasing 38% and 44%, respectively; relative to other propellers. Also, the curve of the efficiency gradient of three propellers in the optimum immersion ratio of 0.40 compared to the advancing coefficient shows that the maximum efficiency gradient occurs in the range of 0.7 to 0.9.

doi: 10.5829/ijee.2023.14.02.06

### INTRODUCTION

Surface-piercing propellers are supercavitation propellers operating on the free surface of water and air. Due to features such as high efficiency, replacing the cavitation phenomenon with ventilation, increasing maneuverability, reducing the resistance of the appendage, and reducing the power required for the propeller rotation, this propeller has been used as the common propulsion system of a high-speed marine vehicle. One of the main steps in designing a surface-piercing propeller is to determine the propeller's thrust, torque, and efficiency. These values are obtained from hydrodynamic coefficients with the help of experimental, analytical, and numerical methods. Despite developing numerical and analytical methods, experimental methods are still vital for designing and evaluating surface-piercing propellers under different conditions. Regardless of the development of high-speed vessels and surface-

piercing propulsion systems in this type of vessel, there is still limited experimental data to investigate the propeller's performance in different physical conditions. In 1953, Shiba [1] conducted the first comprehensive experimental study to investigate the effect of Weber number and effective parameters on the ventilation of the semi-submerged propeller in different geometries. The results showed that Weber number of 180 is the critical Weber number of the surface piercing propeller to scale the results from the model to the real prototype and the effect of this parameter on values greater than 180 on the hydrodynamic coefficients of the propeller and its ventilation is insignificant. In 1968, Hadler [2] investigated two three-bladed propellers and one two-bladed supercavitation propeller with different diameters and the same expanded area ratio at different advance ratios. According to their results, the surface piercing propeller has two areas: basic ventilation and full ventilation. Due to the formation of the ventilation

\* Corresponding author email: [rshafaghat@nit.ac.ir](mailto:rshafaghat@nit.ac.ir) (R. Shafaghat)

phenomenon a high lift-to-drag ratio, higher efficiency is obtained in the basic ventilation area. Alder and Moore [3] in 1977 studied an 8-blade surface-piercing propeller to investigate the effect of yaw angle on the performance of the surface-piercing propeller. In the experimental tests, the immersion ratio was equal to 33%, and the inclination shaft angle was 19.5 degrees for all tests. By studying the hydrodynamic performance of the propeller in four different yaw angles, they concluded that by increasing the yaw angle from zero to 19.5 degrees, the efficiency increases by 15%. In 1996, Olofsson [4] conducted an experimental investigation of a 4-bladed surface piercing propeller at different yaw angles and inclination shaft, as well as the immersion ratio of 0.33, to determine the effect of Froude number and cavitation on the hydrodynamic coefficients of the propeller. According to the results, Froude number equal to 4, the critical Froude number of the propeller, was introduced to the scale model results model to the real prototype. In an experimental study in 2000, Dyson [5] investigated three four-bladed propellers and one five-bladed propeller at 0.33 and 0.50 immersion ratios and different yaw angles and inclination shaft angles. Experimental results showed that an increase in the immersion ratio will increase the propeller's thrust and torque, but it does not significantly affect efficiency. In 2002, Fernando et al. [6] investigated four propellers with different pitch ratios in immersion ratios of 0.4, 0.5, 0.6, and 0.7 and different inclination shaft angles. The results showed that the immersion ratio is also one of the effective parameters of Weber number of the propeller. Also, the critical advance coefficient of a surface-piercing propeller is a function of the critical Weber number and pitch ratio. Ferrando et al. [7] in 2007 investigated the effect of the parameters of pitch ratio, blade number, and inclination shaft angle in immersion ratios of 0.4, 0.5, 0.6 and 0.7 on the performance of surface piercing propellers using a systematic series of propellers with 4 and 5 blades were investigated in experimental and semi-empirical relationships were presented to predict the hydrodynamic coefficients of the propeller. According to the results, increasing the pitch ratio in the number of different blades increases the critical advance coefficient as well as the thrust and efficiency of the propeller. In 2009, Ghassemi et al. [8] numerically investigated two surface-piercing propellers in full and partial submergence conditions. The results showed that pitch ratio and Weber number are two effective parameters to distinguish the three ventilation zones of a surface piercing propeller. Also, increasing the pitch ratio will increase the critical advance coefficient of the propeller. In 2012, Misra et al. [9] conducted an experimental investigation of four surface-piercing propellers with different cup shapes in different immersion ratios. According to the results, thrust coefficients and propeller torque will increase with the immersion ratio in constant Weber number. Seyyedi et al. [10] in 2018 investigated a 5-blade surface piercing

propeller in different immersion ratios and yaw angles. Their results showed that increasing thrust ratio and propeller torque increase, but it has slight effect on efficiency. Also, the propeller's critical advance coefficient decreases with the immersion ratio increase. In 2019, Ganji Rad et al. [11] conducted a numerical study of a five-blade surface piercing propeller to investigate the effect of immersion ratio on the ventilation parameter and hydrodynamic coefficients. The results showed that increased immersion ratio caused growths the propeller torque and thrust. But the critical advance coefficient of the propeller decreased. Also, the propeller experiences higher efficiency in high advance coefficients and low immersion ratio. Yousefi and Shafaghat [12] in 2020 numerically investigated the ventilation parameter of a five-blade surface piercing propeller at different radial positions of the blade. They introduced two parameters of ventilation length and thickness to describe this phenomenon. According to the results, in constant advance coefficients, the thickness and length of the ventilation area decreased with an increase in the radius ratio. In 2020, Seyyedi and Shafaghat [13] conducted a statistical review of analytical and numerical experimental studies. In this review, important geometrical and physical parameters were introduced in theoretical and experimental studies, and a comprehensive overview of the future research in the field of surface-piercing propeller was presented. In 2021, Bushehri and Haghghi [14] conducted an experimental and numerical investigation of a five-blade surface-piercing propeller. In this experimental investigation, the efficiency of the propeller was evaluated at different operating conditions of a catamaran vessel in sea trials. The results show that despite the low speed of the vessel and the lower efficiency of the propeller before the planning phase (submerged mode), the thrust and torque of the propeller are greater than the first stage of the semi-planning phase (semi-submerged mode). Past experimental studies show that in designing and selecting a surface piercing propeller, using the model test results in open water experimental conditions is a more appropriate method, despite the higher cost compared to numerical methods. The model size is considered one of the important issues in the experimental investigation process. The free surface water tunnel is a widely used facility in experimental tests of surface-piercing propellers. The model size in water tunnel tests is usually effective on the accuracy of the measuring equipment and the possibility of better detection of hydrodynamic phenomena; in such a way that the model size is considered as large as possible. But increasing the size of the model due to the limitations of the test section can lead to adverse effects such as blockage and wall effects and reduce the accuracy of the results. Therefore, choosing the optimal size of the model plays an important role in the possibility of scaling the results from the model to the real prototype. In the present work, the effects of

scaling on the hydrodynamic coefficients of a semi-submerged propeller have been investigated. For this purpose, three propellers with the same pitch ratio and different diameters in the range of advance coefficients (0.4-1.05) and four immersion ratios (0.4-0.7) have been experimentally investigated.

**Effective parameters in the design**

The hydrodynamic coefficients of thrust, torque and efficiency of a propeller depend on various parameters. In submerged propellers, these coefficients are diameter (D), pitch (P), number of blades (Z), extended area ratio (EAR), rake angle ( $\theta_r$ ), skew angle ( $\theta_s$ ), blade thickness (t), cross-section profile type (f) and dimensionless Reynolds numbers (Re), advance coefficient (J), Froude (Fr) and cavitation ( $\sigma$ ) are dependent. According to the functional conditions of the surface piercing propeller and the splitting of the water surface in each round of rotation, the four parameters of Weber number (We), immersion ratio (I), inclination shaft angle ( $\gamma$ ) and yaw angle ( $\Psi$ ) in addition to the parameters mentioned for propellers. Common submerged will affect the hydrodynamic coefficients of this type of propellers [8]. Figure 1 shows different angular conditions of a surface-piercing propeller.

The parameters affecting the hydrodynamic coefficients of thrust and torque of a surface-piercing propeller can be defined as follows (Equation (1)) [13, 15]:

$$K_T \text{ and } K_Q = f(D, P/D, Z, EAR, J, \theta_s, \theta_r, t, f, Re, \sigma, We, I_T, \gamma, \Psi) \quad (1)$$

Dimensionless parameters are defined by Equation (2) [16]:

$$\begin{aligned} Fr &= \frac{n \cdot D}{\sqrt{g \cdot D}} & J &= \frac{V_A \cos(\gamma)}{nD} \\ We &= \sqrt{\frac{n^2 \cdot D^3}{\kappa}} & Re &= \frac{n \cdot D^2 \cdot EAR}{\nu \cdot Z} \\ I &= \frac{h_T}{D} \end{aligned} \quad (2)$$

$\kappa$  and  $\nu$  are the dynamic surface tension and kinematic capillary of water,  $h_T$  is the immersion height of the propeller and  $n$  is the rotational speed of the propeller.  $\kappa$  is defined by  $\kappa = \sigma/\rho$ , where  $\rho$  and  $\sigma$  are the volume averaged density and surface tension coefficient

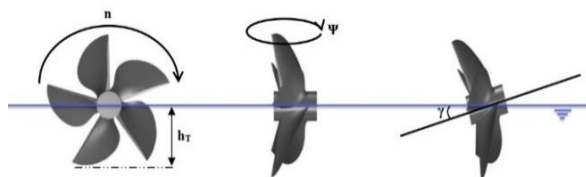


**Figure 1.** Location of a surface-piercing propeller in different angular conditions

respectively. The hydrodynamic coefficients of the propeller are defined as follows (Equation (3)):

$$K_T = \frac{T}{\rho n^2 D^4} \quad K_Q = \frac{Q}{\rho n^2 D^5} \quad \eta = \frac{J}{2\pi} \cdot \frac{K_T}{K_Q} \quad (3)$$

T is thrust, Q is torque, and  $\rho$  is water density. Table 1 shows the parameters used in Equations (1), (2) and (3).

**Laboratory and calibration equipment**

As mentioned, the free surface water tunnel has been used for the experimental tests (Figure 2). Two views of the propeller installed in the test section are shown in Figure 3. The flow velocity in the test section and thrust and propeller torque are the most important parameters measured in each run. A two-component propeller dynamometer (Figure 4) measures thrust and torque. Applying different functional test conditions makes it possible to change the inclination shaft angle and the immersion ratio. The general specifications of the free surface tunnel and the measuring equipments are presented in Table 2 [17]. LabVIEW software is used for data acquisition and post-processing of output data (Figure 5).

**Table 1.** Parameters used in the equation

| Parameter | Name                              |
|-----------|-----------------------------------|
| J         | Advance coefficient               |
| $V_A$     | Advance velocity                  |
| D         | Diameter                          |
| $h_T$     | Immersion height of the propeller |
| n         | Rotational speed of the propeller |
| Fr        | Froude number                     |
| We        | Weber number                      |
| EAR       | Expanded area ratio               |
| $\gamma$  | Shaft inclination angle           |
| $\nu$     | Kinematic viscosity               |
| $\kappa$  | Kinematic capillary               |
| Re        | Reynolds number                   |
| I         | Immersion ratio                   |
| g         | Gravity acceleration              |
| Z         | Number of blades                  |
| T         | Thrust                            |
| Q         | Torque                            |
| $\rho$    | Density                           |
| $K_T$     | Thrust coefficient                |
| $K_Q$     | Torque coefficient                |
| $\eta$    | Efficiency                        |



Figure 2. A view of the free surface water tunnel of Noshirvani University of Technology, Babol, Iran [18]



Figure 3. Front and top view of a surface piercing propeller in the test section



Figure 4. A view of the dynamometer used to measure the hydrodynamic coefficients of thrust and torque

Before the tests, all measuring equipment's calibrated. For the speed calibration of the test section, the results obtained from the manometric speedometer of an ultrasonic flow meter (Fluxus ADM 6725, Flexim Company) were used. Also, uncertainty analysis was performed by equations reported in literature [19, 20] to check the reliability of the velocity measurement test section. According to the defined uncertainty analysis equations and the existing errors, 6 repetitions were considered for speed measurement. The standard

Table 2. General specifications of the free surface water tunnel and the test section [17]

| Part         | Parameter                          | Value  |
|--------------|------------------------------------|--------|
| Test section | Length(m)                          | 2      |
|              | Width(m)                           | 0.3    |
|              | Height(m)                          | 0.3    |
|              | Maximum speed in test section(m/s) | 5      |
| Nozzle       | Contraction area ratio             | 9 to 1 |
| Pump         | Power(kw)                          | 45     |
|              | Maximum rotational velocity(rpm)   | 3600   |
| Dynamometer  | Maximum thrust(N)                  | 981    |
|              | Maximum torque(N.m)                | 67     |

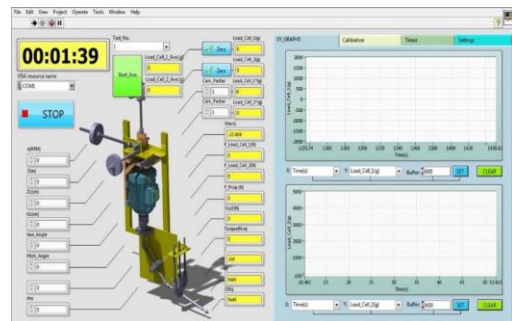


Figure 5. A view of the software LabVIEW [17]

deviation and coefficient of variation for the flow velocity in the test section are given in Table 3 [21]. The standard deviation is equal to 0.0635.

In the next step, the tests are repeated to calibrate the thrust and torque sensors of the tunnel dynamometer and to ensure the accuracy of the extracted results in four stages of repetition for one of the propellers. Table 4 shows the results of thrust and torque coefficients in two advance coefficients and a fixed immersion ratio of 0.40 for a propeller with a diameter of 0.125 meters. As can be seen, the difference for the thrust coefficient and the torque in the advance coefficient is equal to 0.9, respectively 0.00139 and 0.0038, which indicates the acceptable accuracy of the obtained results.

### Characteristics of model propellers

The propellers of the model are made of PLA plastic; their geometric specifications are presented in Table 5. The scale ratio of the reference propeller (diameter 0.125 m) with propellers 0.132 m and 0.140 m equals 1.056 and

Table 3. Calculation of the standard deviation of the speed data in the test section [21]

| Height | Test 1 (m/s) | Test 2 (m/s) | Test 3 (m/s) | Test 4 (m/s) | Test 5 (m/s) | Test 6 (m/s) | Average | Standard deviation | Coefficient of variation |
|--------|--------------|--------------|--------------|--------------|--------------|--------------|---------|--------------------|--------------------------|
| 19     | 1.854        | 1.80         | 1.836        | 1.871        | 1.719        | 1.723        | 1.803   | 0.0635             | ±0.0259                  |

**Table 4.** Calibration of thrust and torque sensors in two advance coefficients [21]

|                    | Advance coefficient | Number | Test 1 | Test 2 | Test 3 | Test 4 | Average | Standard deviation | Coefficient of variation |
|--------------------|---------------------|--------|--------|--------|--------|--------|---------|--------------------|--------------------------|
| Thrust coefficient | 0.9                 | 4      | 0.0369 | 0.0372 | 0.0399 | 0.0375 | 0.038   | 0.00139            | 0.0007                   |
|                    | 0.599               | 4      | 0.0467 | 0.0440 | 0.0407 | 0.0498 | 0.045   | 0.0038             | 0.0019                   |
| Torque coefficient | 0.9                 | 4      | 0.1561 | 0.1660 | 0.1261 | 0.2059 | 0.1665  | 0.0329             | 0.0164                   |
|                    | 0.559               | 4      | 0.1324 | 0.1254 | 0.1177 | 0.1997 | 0.1438  | 0.0377             | 0.0188                   |

1.12, respectively. Figure 6 shows a view of the propeller with a diameter of 0.125 m.

In order to determine the hydrodynamic coefficients of the propeller, experimental tests were performed in fourteen advance coefficients [0.4-1.05] and four immersion ratios [0.4-0.7] (Table 6).

**Test conditions**

One of the limitations of conducting experimental tests of surface piercing propellers is the independence of experimentally results from the effect of Reynolds,

Froude and Weber dimensionless numbers. It will be necessary to satisfy the laws of similarity to generalize the experimental results of the model to the real prototype in the tests of the propeller in the free surface water tunnel. The values of the mentioned dimensionless numbers must be higher than the defined critical values to satisfy the similarity rule. In this situation, the effect of these numbers on the hydrodynamic coefficients and operational conditions of the propeller can be ignored. According to the experimental results of Olofsson [4] and Shiba [1], if Froude number is greater than 4, it will not affect the hydrodynamic coefficients of the propeller and its advance coefficient during the different phases of the propeller ventilation; as the ventilated bubbles approach their final shape, the results can be considered independent of Froude number. Also, Shiba [1] declared the critical Weber number equal to 180 to generalize the model's results to the real prototype. At values higher than 180, the critical advance coefficient and the propeller ventilation parameter will be independent of the effect of Weber number. In 2007, to generalize the results of the model to the real prototype, Pustoshny et al. [22] determined the limits of Reynolds, Froude and Weber numbers (Equation (4)).

**Table 5.** Geometric specifications of model propellers

| Parameter           | Symbol | Value |      |      |
|---------------------|--------|-------|------|------|
| Diameter (mm)       | D      | 125   | 132  | 140  |
| Hub diameter (mm)   | d      | 25    | 26.4 | 28   |
| Hub diameter ratio  | d/D    | 0.2   | 0.2  | 0.2  |
| Number of blades    | Z      | 5     | 5    | 5    |
| Pitch ratio in 0.7R | P/D    | 1.46  | 1.46 | 1.46 |
| Rotation direction  | -      | RH    | RH   | RH   |



**Figure 6.** A view of propeller

$$\begin{aligned}
 Re &= \frac{n \cdot D^2 \cdot (A_E / A_0)}{\nu \cdot Z} \geq 5 \times 10^5 \\
 Fr &= n \cdot \sqrt{\frac{D}{g}} \geq 3.5 \\
 We &= \sqrt{\frac{\rho \cdot n^2 \cdot D^3}{\sigma}} \geq 180
 \end{aligned}
 \tag{4}$$

According to the mentioned critical values, for three propellers with diameters of 0.125m, 0.132 m and 0.140m, the rotational speed has been determined as 34.8, 33 and 31 revolutions per second, respectively.

**Validation of the results**

The experimental results were validated with Seyyedi et al. [10]. For this purpose, experimental tests were performed on a five-bladed propeller with a diameter of 0.132 m and an immersion ratio of 0.40. The comparison of the results related to the hydrodynamic coefficients of thrust and torque is shown in Figure 7. As can be seen, the error percentage of the average experimental results obtained for the torque and thrust coefficients is 4.57%

**Table 6.** The range of investigated parameters

| Parameter           | Symbol         | Value  |
|---------------------|----------------|--|
| Advance coefficient | J              | 0.4-0.45-0.5-0.55-0.6-0.65-0.7-0.75-0.8-0.85-0.9-0.95-1-1.05 |
| Immersion ratio     | I <sub>T</sub> | 0.4-0.5-0.6-0.7  |



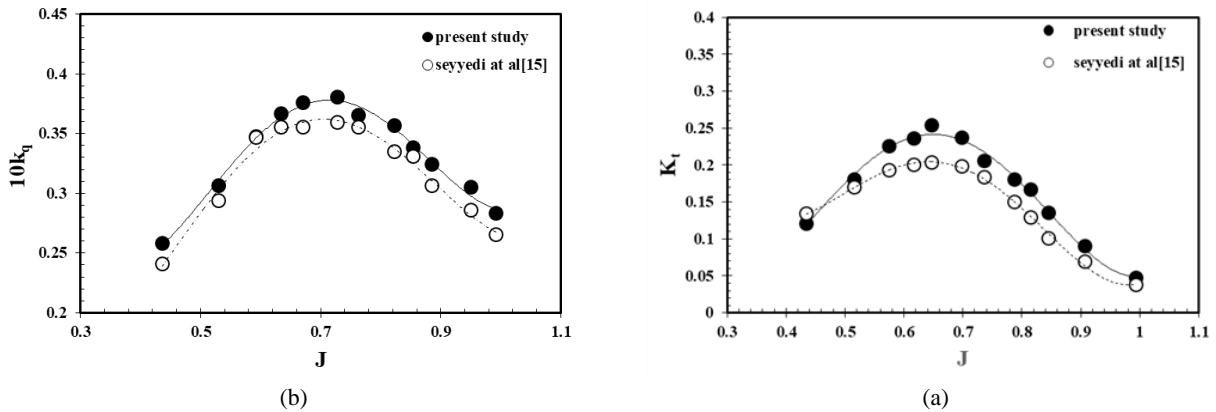


Figure 7. Comparison of (a) thrust (b) torque coefficients with the results of Seyyedi et al. [10]

and 8%, respectively; which indicates that the results are in good agreement with the projected model.

The effects of scaling on the hydrodynamic coefficient of three propellers with diameters of 0.125m, 0.132 m and 0.140 m were investigated (Figure 8). According to Beykani et al. [21], with an increase in propeller immersion and as a result of the blockage ratio, the amount of thrust of the propeller does not experience much changes. Figure 8 shows the torque coefficient curves of three propellers with diameters of 0.125 m, 0.132 m and 0.140 m in different immersion ratios. By increasing the amount of immersion in different advance coefficients, the torque of the 0.140 m propeller experiences a significant decrease compared to the other two propellers. One of the important issues in an experimental study is to get a proper insight into the effect of variable parameters on the outputs corresponding to the experimental model.

In the following, the effect of changes in the advance speed on the performance of all three propellers in different immersion ratios is investigated. Also, considering the importance of the blockage ratio

parameter and the influence of this parameter on the hydrodynamic coefficients of the semi-submerged the propeller, the thrust, and the torque coefficients of all three propellers in different submersion ratios have been investigated and analyzed. The gradient efficiency of all three propellers in the optimal immersion ratio to the advance coefficients has also been investigated.

## RESULTS AND DISCUSSION

One of the essential parameters in the physical conditions of a surface-piercing propeller is the immersion ratio. Figure 9 shows the 3D diagram of the trust coefficients of three propellers with a diameter of 0.125 m, 0.132 m and 0.140 m relative to the advance speed in the different immersion ratios. As it can be seen, the amount of thrust coefficient of three propellers in different immersion ratios and forward speeds are in good agreement. Also, with the immersion ratio increase, the three propellers' production thrust increases at different advanced speeds; In such a way that by increasing the immersion ratio from

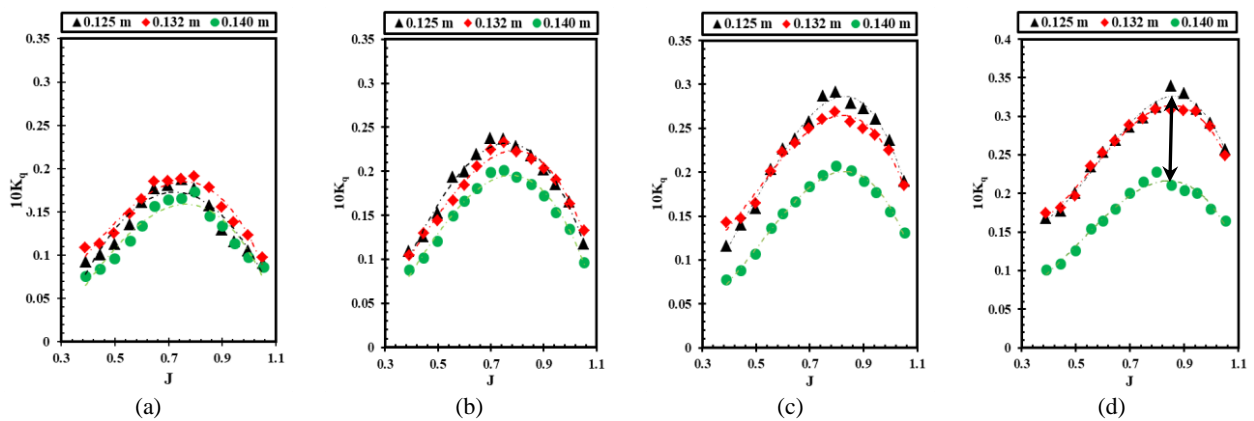
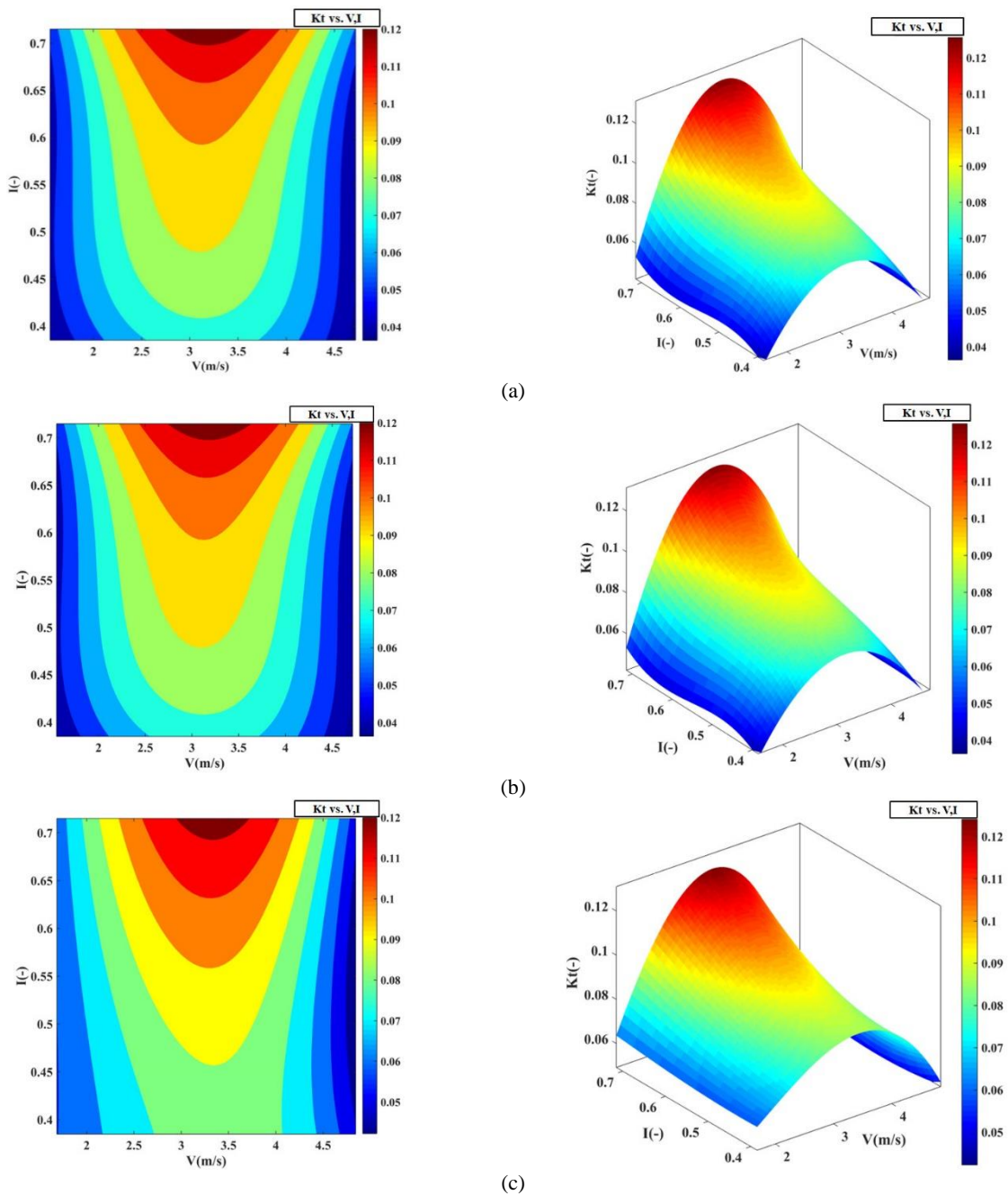


Figure 8. The value of the torque coefficient of three propellers in immersion ratios a) 0.40, b) 0.50, c) 0.60, d) 0.70 [20]

0.40 to 0.70, the maximum amounts of thrust coefficient for propellers with diameters of 0.125 m, 0.132 m, and 0.140 m are equal to 30.2%, 33.3%, and 39.62%, respectively. According to the changes in the thrust coefficient curve, the critical advance velocity of three propellers is in the range of 3 to 3.5 m/s. According to the definition of the ventilation range of a propeller, this speed range is equivalent to the transmission area of the propeller. Therefore, the ventilation of the propeller is

independent of an increase in the diameter of the model in an experimental test. The maximum thrust coefficient of three propellers occurs at the immersion ratio of 0.70. Hydrodynamic coefficients of torque of the propeller with a diameter of 0.125 m, 0.132 m and 0.140 m relative to different advancing speeds in immersion ratios are shown in Figure 10. As can be seen, with an increase in immersion ratio from 0.40 to 0.70, the amount of torque of three propellers increases. Also, according to the



**Figure 9.** Curve thrust coefficients of propellers with diameter a) 0.125 m, b) 0.132 m, c) 0.140 m at advancing speeds and different immersion ratios

results, the torque of two propellers with a diameter of 0.125 m and 0.132 m have a good match in different immersion ratios, propellers. Two propellers with a diameter of 0.125 m and 0.132 m experience an average increase in more than 50% for the maximum torque coefficient by increasing the immersion ratio from 0.40 to 0.70. While an increase in the maximum value of the propeller torque coefficient with a diameter of 0.140 m is almost 37%. In other words, the torque of the propeller with a diameter of 0.140 m increases, unlike the two

propellers with a lower slope. The influence of the blockage ratio on the propeller torque causes this decrease in slope. However, maximum torque coefficient of three propellers occurs in immersion ratio of 0.70.

Figure 11 shows the effect of the immersion ratio parameter on the hydrodynamic efficiency coefficient of the propeller with a diameter of 0.125 m, 0.132 m and 0.140 m. As it can be seen, with an increase in the immersion ratio, the efficiency coefficient of all three propellers follows an increasing slope and the amount of

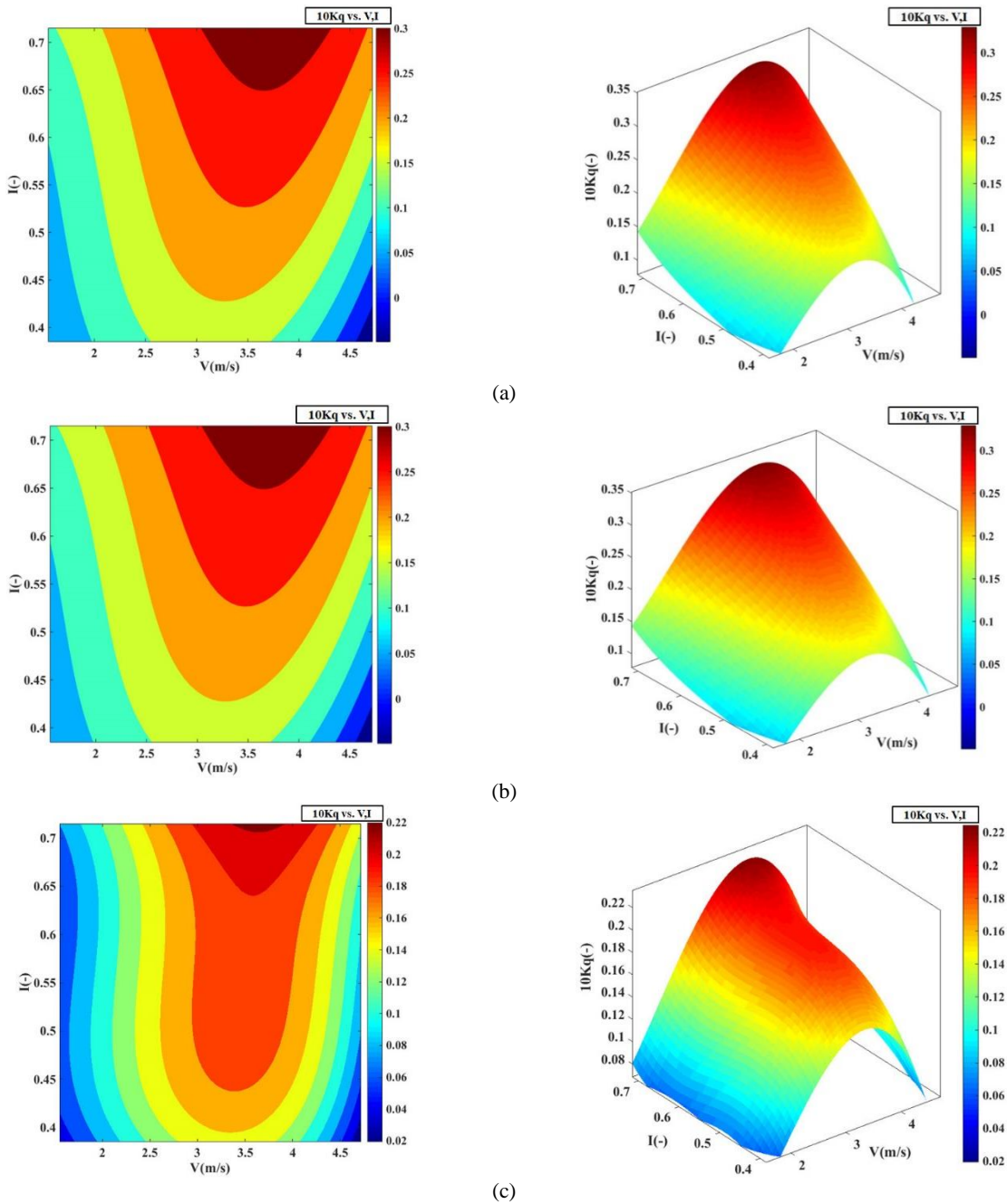


**Figure 10.** torque coefficient curve of propellers with diameter a) 0.125 m, b) 0.132 m, c) 0.140 m at advancing speeds and different immersion ratios



efficiency changes decreases at high forward speeds and the maximum efficiency of three propellers occurs at the immersion ratio of 0.40. Also, by increasing the immersion ratio, the propeller's efficiency with a diameter of 0.140 m will be different compared to the other two propellers. With an increase in immersion ratio and as a result of the effect of wall effects, the amount of torque of the propeller with a diameter of 0.140 m experiences a lower increasing slope than the other two propellers.

Therefore, according to the inverse relationship between the torque coefficient and the efficiency of open water, the efficiency of the propeller with a diameter of 0.140 m will be higher than the other two propellers in immersion ratio 0.60 and 0.70. Such that by increasing the immersion ratio from 0.60 to 0.70, the maximum efficiency of the propeller with a diameter of 0.140 m will experience a very small increase, while the two propellers will experience an average decrease of 9%.

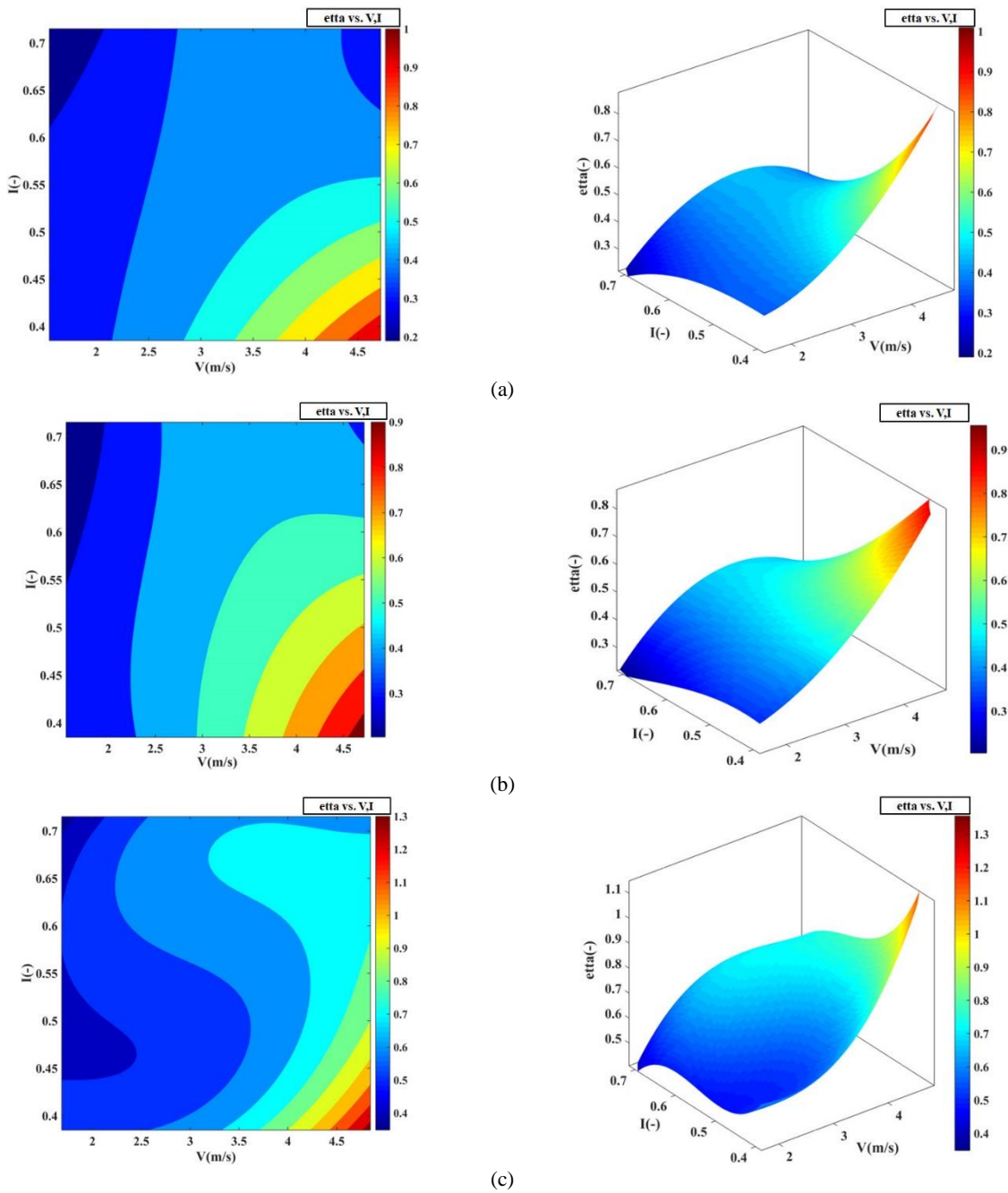


**Figure 11.** efficiency coefficient curves of propellers with diameter a) 0.125 m, b) 0.132 m, c) 0.140 m at advancing speeds and different immersion ratios

According to the results, it can be seen that increasing the immersion ratio generally increases the torque and thrust of a surface-piercing propeller. By increasing the immersion ratio, the level of propeller submerged increases, and due to the pressure nature of the propeller thrust force and increasing the pressure difference of the face and back surface of the blade, the amount of thrust produced by the propeller increases. Also, by increasing the immersion ratio, the duration of the presence of the propeller in the air-fluid has decreased, so the propeller needs more torque to achieve a certain rotational speed. As mentioned in the curves corresponding to the torque coefficient of the three propellers by diameter 0.125 m, 0.132 m, and 0.140 m at different advance speeds and immersion ratios, it is expected that the torque of the three propellers is equal in different immersion ratios. However, by increasing the immersion ratio from 0.40 to 0.70, the propeller's torque with a diameter of 0.140 m is less than the other two propellers. Increasing the immersion ratio will increase the blockage ratio parameter, which will affect the experimental results of a surface-piercing propeller. So, the three-propeller blockage ratio parameter on hydrodynamic coefficients of thrust, torque and efficiency was investigated.

One of the limitations of performing the test in a water tunnel is the phenomenon of blockage and the adverse effects of the tunnel wall in the test section on the corresponding outputs of the experimental test. The effect

of this phenomenon is measured by a concept called blockage ratio. The ratio of the area of the propeller disc to the area of the tunnel test cross section is called the blockage ratio (Equation (5)). Due to the functional conditions of the surface-piercing propeller and the possibility of changing the amount of propeller immersion, this parameter has not had a single value and varies in different immersion ratios. In Table 7, the blockage ratio of three propellers models is shown to be diameter 0.125 m, 0.132 m and 0.140 m in different immersion ratios. Increasing the immersion ratio increases the blockage ratio in all three propellers.

$$B = \frac{A_{\text{blockage}}}{A_{S,T}} \tag{5}$$

In Figure 12, the thrust coefficient curve shows three propellers with diameters of 0.125 m, 0.132 m and 0.140 m relative to the advancing coefficient and blockage ratio.

**Table 7.** Percentage of blockage ratio of three non-aluminum propellers in different immersion ratios

| Diameter(m) | Immersion ratio |       |       |       |
|-------------|-----------------|-------|-------|-------|
|             | 0.40            | 0.50  | 0.60  | 0.70  |
| 0.125       | 7.63            | 10.22 | 12.81 | 15.29 |
| 0.132       | 8.51            | 11.40 | 14.28 | 17.05 |
| 0.140       | 9.58            | 12.82 | 16.07 | 19.18 |

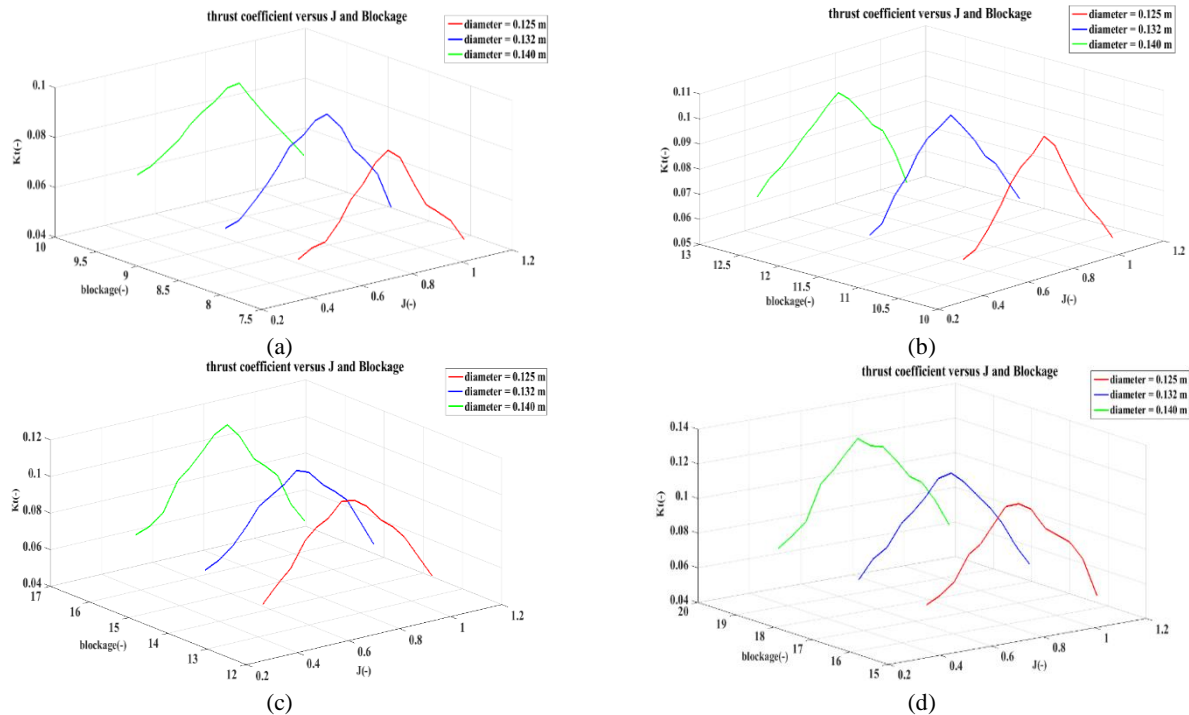


**Figure 12.** The curve of the three-propeller thrust coefficient relative to the advancing coefficient in different immersion ratios a) 0.40, b) 0.50, c) 0.60, d) 0.70

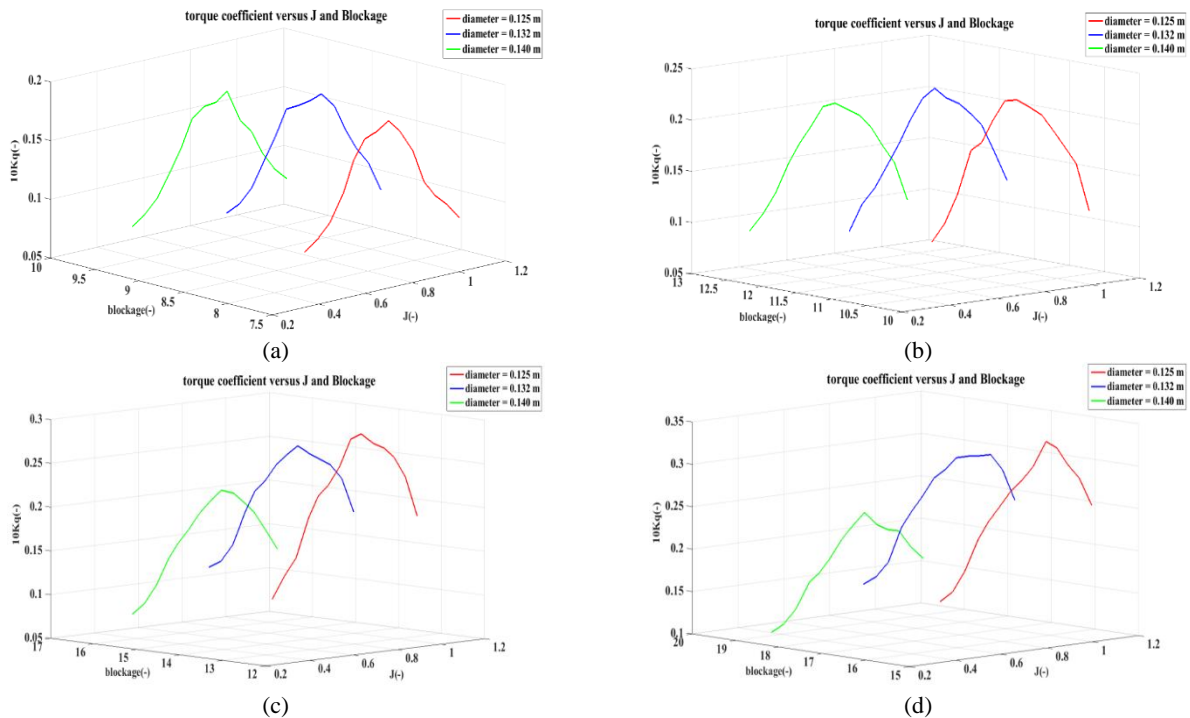
As can be seen, with the increase in the blockage ratio, the amount of thrust produced by the three propellers in different blockage ratios is relatively consistent with each other. However, the amount of thrust coefficient in the blockage ratios corresponding to the immersion ratio of 0.60 and 0.70 for the propeller by diameter 0.140 m is slightly different from the other two propellers.

In Figure 13, the torque coefficient curves of the three propellers are shown to diameter 0.125 m, 0.132 m and 0.140 m compared to the advancing coefficients and different blockage ratios. As can be seen, the torque of the three propellers in the immersion ratios of 0.40 and 0.50 is appropriate, but with increasing the blockage ratio, the torque of the propeller with diameter 0.140 m decreases compared to the other two propellers. In a way that in the 19.18 blockage ratio corresponding to the immersion ratio of 0.70, Maximum torque of the propeller with a diameter of 0.140 m experiences a 33% reduction to that of the propeller with a diameter of 0.125 m.

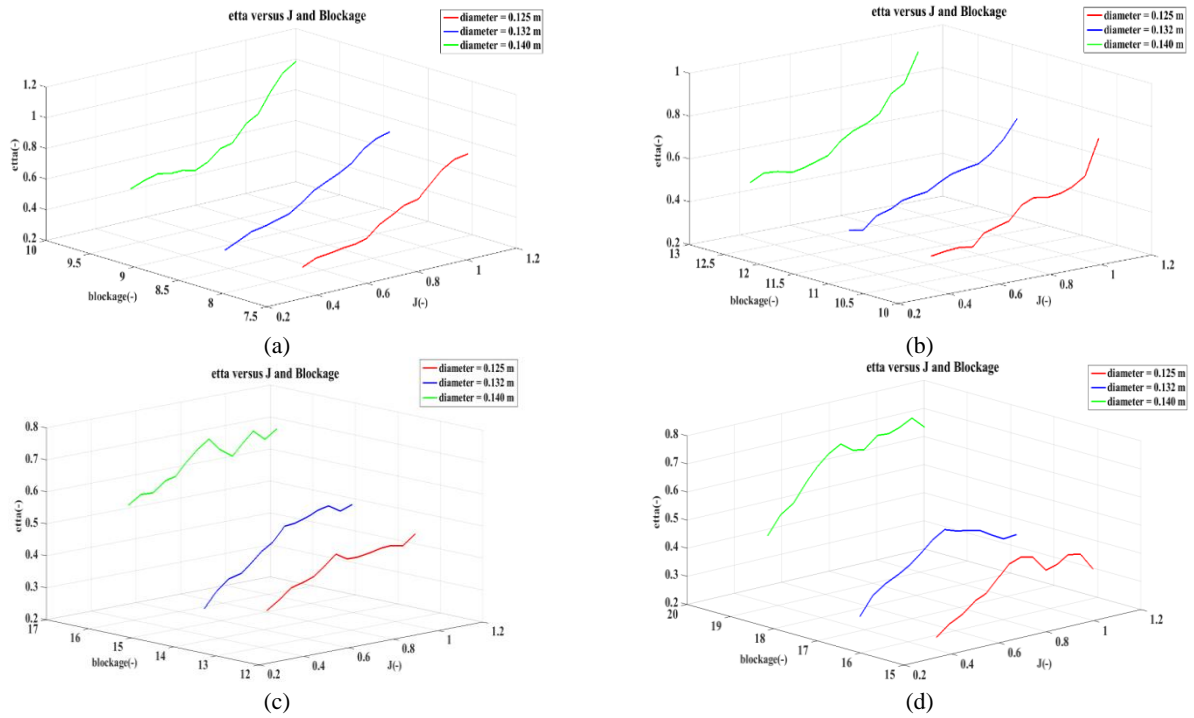
Figure 14 shows the efficiency of three propellers with diameters of 0.125 m, 0.132 m and 0.140 m in relation to advance coefficients and different blockage ratios. As can be seen, with increasing the blockage ratio to 20, the difference efficiency propeller by diameter 0.140 m increases with the other two propellers. The efficiency of the propeller is inversely related to its torque coefficient. Due to the decrease in the torque coefficient of 0.140 m due to increasing the blockage ratio and its proximity to 20, the efficiency propeller with diameter

0.140 m experiences a significant increase with increasing the blockage ratio. Also, The maximum value of the propeller with a diameter of 0.140 m in immersion ratios of 0.60 and 0.70 will experience an increase in 38% and 44%, respectively, compared to the maximum value of the other two propellers.

According to Figure 14, the maximum efficiency of three propellers occurs in an immersion ratio of 0.40. Therefore, the changes in the efficiency of the three propellers in the immersion ratio of 0.40 are investigated. In Figure 15, the efficiency gradient of the propeller with a diameter of 0.125 m in the ratio of 0.40 is shown. In order to investigate the gradient efficiency of the propeller in different advancing coefficients, the unit value is considered as the basis of intense changes. In this way, in values equal to or greater than 1, the efficiency value has experienced a significant increase; in values less than 1, the increase in the efficiency is less. In the propeller with Diameter 0.125 m, the rate of efficiency changes in the range of 0.4 to 0.6 is less than 1 and the propeller efficiency does not experience significant growth in this section. In the advancing coefficient of 0.7, the propeller efficiency increases suddenly, representing the value of changes greater than 1. The trend of increasing efficiency in advancing coefficient values greater than 0.7 is fewer slopes so that it decreases sharply in the advancing coefficient of 0.85. Then, the efficiency of a sharp increase occurs in the advancing coefficient values of 0.95 and 1.



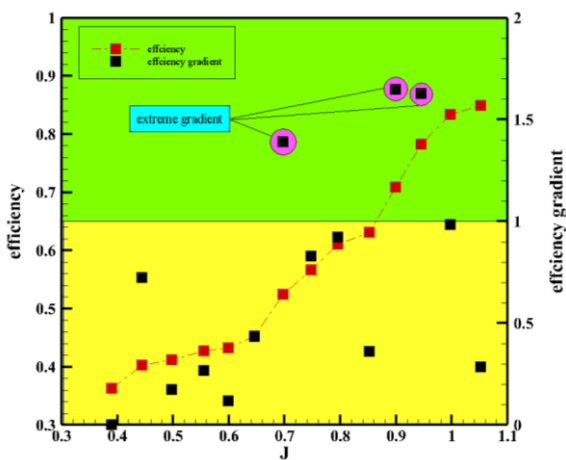
**Figure 13.** The curve of the three-propeller torque coefficient relative to the advancing coefficient in different immersion ratios a) 0.40, b) 0.50, c) 0.60, d) 0.70



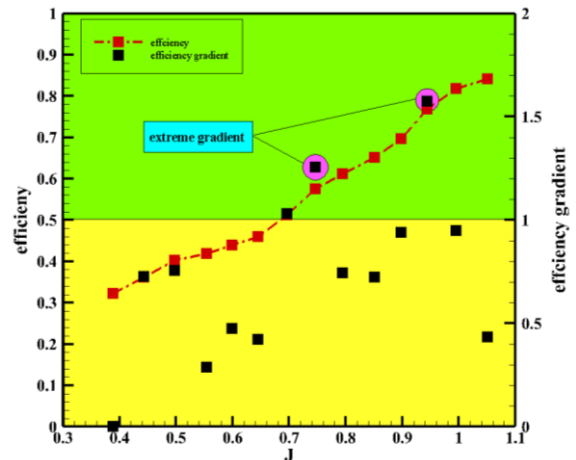
**Figure 14.** The curve of the three-propeller efficiency coefficient relative to the advancing coefficient in different immersion ratios a) 0.40, b) 0.50, c) 0.60, d) 0.70

Figure 16 shows the efficiency curve and its gradient in different advancing coefficients and an immersion ratio of 0.40 for the propeller with diameter 0.132 m. As can be seen, the propeller efficiency curve with a diameter of 0.132 m experiences three peaks at advancing values of 0.7, 0.75 and 0.95. In such a way, in the range of 0.6 to 0.75, the efficiency experiences a sharp rise to the maximum peak of 0.75 and then suffers a sharp drop. In this period, the thrust and torque of the propeller follow the uptrend, but the trend

of trust increase is more severe than the torque. Then, in the range of 0.8 to 0.95, the efficiency curve again follows an increasing trend to the maximum peak of 0.95. In the range of 0.8 to 0.95, the propeller torque has a downward trend with a steep slope, while in this period the decrease slope of the propeller thrust is less. Therefore, the efficiency will have a severe incremental slope. Also maximum changes in the propeller efficiency with a diameter of 0.132 m occur in the range of 0.8 to 0.95.



**Figure 15.** Efficiency curve and its gradient relative to the advancing coefficient for the propeller with a diameter of 0.125 m in the immersion ratio of 0.40



**Figure 16.** Efficiency curve and its gradient relative to the advancing coefficient for the propeller with a diameter of 0.132 m in the immersion ratio of 0.40

The efficiency curve and its gradient for the propeller with a diameter of 0.140 m compared to different advancing coefficients in the immersion ratio of 0.40 in Figure 17 are shown. As can be seen, the propeller efficiency in the range of 0.6 to 0.7 follows a severe incremental trend. As can be seen, the propeller efficiency in the range of 0.6 to 0.7 follows a severe incremental trend. Then, from 0.7 to 0.85, the propeller efficiency has a severe fluctuation and experiences instantaneous increase and decrease. In the advancing coefficient of 0.95, the maximum changes in the efficiency propeller occur. In this advance coefficient thrust and torque of the propeller both have a downtrend, but the downtrend of torque is severe and the torque reduction is more severe than thrust in the advancing coefficient of 0.85. Therefore, efficiency will maximum experience its change.

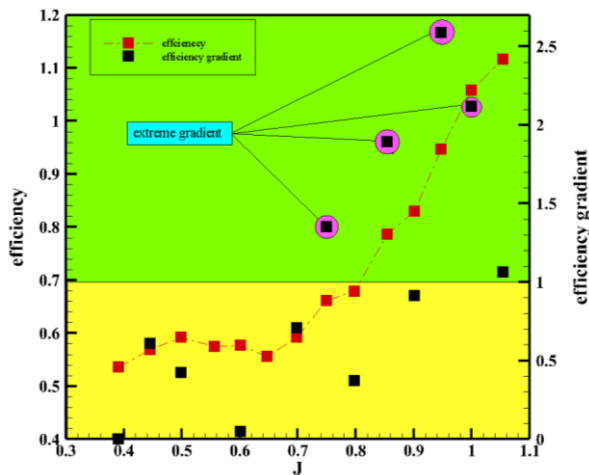


**Figure 17.** Efficiency curve and its gradient relative to the advancing coefficient for the propeller with a diameter of 0.140 m in the immersion ratio of 0.40

## CONCLUSION

This paper investigates two parameters of immersion ratio and wall obstruction ratio in three propellers with the same pitch ratio, expanded area, and different diameter. In order to produce geometry of propellers have been used of 3D printer machine. The material of the model propellers is made of PLA. Also, in order to perform the test, the free surface water tunnel of Babol Noshirvani University of Technology (Babol, Iran) has been used. Considering the importance of investigating the speed of the test in an experimental study, the hydrodynamic coefficients of three propellers of four immersion ratios to different advancing speeds were investigated. Also, the importance of the effect of wall blockage and its effect on the hydrodynamic function of three propellers to advance speed was investigated.

Finally, considering the importance of propeller efficiency as the determinant of its selection, the efficiency gradient of the three propellers in the optimal immersion ratio investigated. The obtained results can be summarized as follows:

- Investigation of the hydrodynamic coefficients of three propellers at different advance speeds shows that three propellers' maximum coefficient of thrust occurs in different immersion ratios in the speed range of 3-3.5 m/s. In fact, in experimental tests, the transfer area of three propellers occurs in this range.
- By increasing the immersion rate of the three propellers and consequently increasing the blockage ratio, the torque produced by the propeller with a diameter of 0.140 m decreases compared to the other two propellers, while the propeller thrust 0.140 m does not have a significant difference with the other two propellers. Due to the inverse relationship between the torque produced by the propellers and its efficiency, by increasing the blockage ratio, the efficiency of the propellers with a diameter of 0.140 m is significantly increased compared to the other two propellers.
- By increasing the propeller advancing coefficient, the rate of change in the propeller's efficiency increases. The maximum gradient occurs in the range of advance coefficient 0.7 to 0.9, representing the transfer zone of the three propellers.
- According to the definition of the blockage ratio for a model in experimental conditions and also the performance conditions of the surface-piercing propeller, in this type of propeller, the blockage ratio has a direct relationship with the immersion ratio. By increasing the blockage ratio to more than 17%, the influence of this parameter on the torque coefficient of the surface-piercing propeller increases.

## REFERENCES

- Shiba, H., 1953. Air-drawing of marine propellers. *Report of transportation technical research institute*, 9, pp.1-320.
- Hadler, J.B., 1968. Performance of partially submerged propellers. 7th ONR Symp Nav Hydrodyn 1968).
- Alder, R.S., and Moore, D.H., 1977. Performance of an inclined shaft partially-submerged propeller operating over a range of shaft yaw angles. David W Taylor Naval Ship Research and Development Center Bethesda Md Ship. <https://apps.dtic.mil/sti/pdfs/ADA048359.pdf>
- Olofsson, N., 1996. Force and flow characteristics of a partially submerged propeller. Chalmers University of Technology.
- Dyson, P.K., 2000. Modelling, testing and design, of a surface piercing propeller drive. Doctoral dissertation, University of Plymouth. <https://pearl.plymouth.ac.uk/10026.1/507>
- Fernando, M., Scamardella, A., Bose, N., Liu, P., and Veitch, B., 2002. Performance of a family of surface piercing propellers. *Royal Institution of Naval Architects Transactions Part A International Journal of Maritime Engineering*, 144(Part A1), pp.63-77.



- [http://ecite.utas.edu.au/47284/2/Ferrando\\_RINA\\_Performance](http://ecite.utas.edu.au/47284/2/Ferrando_RINA_Performance)
7. Ferrando, M., Viviani, M., Crotti, S., Cassella, P., and Caldarella, S., 2006. Influence of Weber number on surface piercing propellers model tests scaling. In: Proceedings of 7th international conference on hydrodynamics (ICHHD), Ischia, 4(6).
  8. Ghassemi, H., Shademani, R., and Ardeshtir, A., 2009. Hydrodynamic Characteristics of the Surface-Piercing Propeller for the Planing Craft. In: Volume 4: Ocean Engineering; Ocean Renewable Energy; Ocean Space Utilization, Parts A and B. ASMEDC, pp 589–595. <https://doi.org/10.1115/OMAE2009-79963>
  9. Misra, S.C., Gokarn, R.P., Sha, O.P., Suryanarayana, C., and Suresh, R. V, 2012. Development of a four-bladed surface piercing propeller series. *Naval Engineers Journal*, 124(4). [https://www.imuv.edu.in/Publications/17.Development of a Four Bladed Surface.pdf](https://www.imuv.edu.in/Publications/17.Development%20of%20a%20Four%20Bladed%20Surface.pdf)
  10. Seyyedi, S.M., Shafaghat, R., and Siavoshian, M., 2019. Experimental study of immersion ratio and shaft inclination angle in the performance of a surface-piercing propeller. *Mechanical Sciences*, 10(1), pp.153–167. Doi: 10.5194/ms-10-153-2019
  11. Ganji Rad, R., Shafaghat, R., and Yousefi, R., 2019. Numerical investigation of the immersion ratio effects on ventilation phenomenon and also the performance of a surface piercing propeller. *Applied Ocean Research*, 89, pp.251–260. Doi: 10.1016/j.apor.2019.05.024
  12. Yousefi, A., and Shafaghat, R., 2020. Numerical study of the parameters affecting the formation and growth of ventilation in a surface-piercing propeller. *Applied Ocean Research*, 104, pp.102360. Doi: 10.1016/j.apor.2020.102360
  13. Seyyedi, S.M., and Shafaghat, R., 2020. A review on the Surface-Piercing Propeller: Challenges and opportunities. *Proceedings of the Institution of Mechanical Engineers, Part M: Journal of Engineering for the Maritime Environment*, 234(4), pp.743–770. Doi: 10.1177/1475090220906917
  14. Pakian Bushehri, M., and Golbahar Haghighi, M.R., 2021. Experimental and numerical analysis of Hydrodynamic Characteristics of a surface piercing propeller mounted on high-speed craft. *International Journal of Maritime Technology*, 15, pp.79–91. <http://ijmt.ir/article-1-745-en.html>
  15. Alizadeh Kharkeshi, B., Shafaghat, R., Jahanian, O., Rezanejad, K., and Alamian, R., 2021. Experimental Evaluation of the Effect of Dimensionless Hydrodynamic Coefficients on the Performance of a Multi-Chamber Oscillating Water Column Converter in Laboratory Scale. *Modares Mechanical Engineering*, 21(12), pp.823–834. Doi: <http://dorl.net/dor/20.1001.1.10275940.1400.21.12.5.5>
  16. Alizadeh Kharkeshi, B., Shafaghat, R., Jahanian, O., Alamian, R., and Rezanejad, K., 2022. Experimental study on the performance of an oscillating water column by considering the interaction effects of optimal installation depth and dimensionless hydrodynamic coefficients for the Caspian Sea waves characteristics. *Ocean Engineering*, 256, pp.111513. Doi: 10.1016/j.oceaneng.2022.111513
  17. Shafaghat, R., 2016. Design Algorithm of a Free Surface Water Tunnel to Test the Surface-Piercing Propellers (SPP); Case Study Water Tunnel of Babol Noshirvani University of Technology. *International Journal of Maritime Technology*, 6, pp.19–30. <http://ijmt.ir/article-1-551-en.html>
  18. Deswal, D., Gupta, R., Nandal, P., and Kuhad, R.C., 2014. Fungal pretreatment improves amenability of lignocellulosic material for its saccharification to sugars. *Carbohydrate Polymers*, 99, pp.264–269. Doi: 10.1016/j.carbpol.2013.08.045
  19. Shafaghat, R., Fallahi, M., Alizadeh Kharkeshi, B., and Yousefifard, M., 2022. Experimental Evaluation of the Effect of Incident Wave Frequency on the Performance of a Dual-chamber Oscillating Water Columns Considering Resonance Phenomenon Occurrence. *Iranian Journal of Energy and Environment*, 13(2), pp.98–110. Doi: 10.5829/IJEE.2022.13.02.01
  20. Kharkeshi, B.A., Shafaghat, R., Jahanian, O., Alamian, R., and Rezanejad, K., 2022. Experimental study of an oscillating water column converter to optimize nonlinear PTO using genetic algorithm. *Energy*, 260, pp.124925. Doi: 10.1016/j.energy.2022.124925
  21. Beykani, M., Shafaghat, R., and Yousefifard, M., 2022. Experimental study of scale effect and immersion ratio on the performance characteristics of a surface piercing propeller. *Journal of Marine Engineering*, 18(35), pp.129–140. <http://marine-eng.ir/article-1-943-en.htm>
  22. Pustoshny, A. V, Boitsov, V.P., Lebedev, E.P., and Stroganov, A.A., 2007. Development of 5-blade SPP series for fast speed boat. In: 9th International Conference on Fast Sea Transportation, FAST 2007. pp 348–354.

**COPYRIGHTS**

©2021 The author(s). This is an open access article distributed under the terms of the Creative Commons Attribution (CC BY 4.0), which permits unrestricted use, distribution, and reproduction in any medium, as long as the original authors and source are cited. No permission is required from the authors or the publishers.

**Persian Abstract****چکیده**

در این مقاله به بررسی تاثیر نسبت مغروقیت بر عملکرد هیدرودینامیکی سه پروانه نیمه مغروق با قطرهای ۰/۱۲۵، ۰/۱۳۲ و ۰/۱۴۰ در سرعت‌های پیشروی مختلف پرداخته شده است. آزمون‌های تجربی در تونل آب سطح آزاد دانشگاه صنعتی نوشیروانی بابل صورت پذیرفته است. نتایج نشان می‌دهد که بیشینه ضریب تراست سه پروانه در بازه سرعت پیشروی ۳/۵-۳ متر بر ثانیه روی می‌دهد. این بازه معرف ناحیه انتقال سه پروانه می‌باشد. هم چنین تاثیر نسبت انسداد بر ضرایب هیدرودینامیکی سه پروانه مورد بررسی قرار گرفته است. افزایش میزان غوطه وری سبب افزایش سطح خیس پروانه و در نتیجه افزایش ضرایب هیدرودینامیکی تراست و گشتاور می‌شود اما افزایش قطر پروانه به ۰/۱۴۰ سبب تاثیر گذاری پارامتر نسبت انسداد با افزایش میزان غوطه وری می‌شود و گشتاور پروانه روند کاهشی را تجربه می‌کند؛ به طوری که حداکثر بازده پروانه با قطر ۰/۱۴۰ در نسبت غوطه وری ۰/۶۰ و ۰/۷۰ به ترتیب ۳۴ و ۵۶ درصد نسبت به سایر پروانه ها افزایش می‌یابد. هم چنین منحنی تغییرات بازده سه پروانه در نسبت مغروقیت بهینه ۰/۴۰ نسبت به ضریب پیشروی نشان می‌دهد که در بازه ضریب پیشروی ۰/۷ تا ۰/۹ بیشینه تغییرات بازده رخ می‌دهد.